Observation of $B_s^0 \to \chi_{c1}\phi$ decay and study of $B^0 \to \chi_{c1,2}K^{*0}$ decays ☆

LHCb Collaboration

Abstract

The first observation of the decay $B_s^0 \to \chi_{c1}\phi$ and a study of $B^0 \to \chi_{c1,2}K^{*0}$ decays are presented. The analysis is performed using a dataset, corresponding to an integrated luminosity of 1.0 fb^{-1}, collected by the LHCb experiment in pp collisions at a centre-of-mass energy of 7 TeV. The following ratios of branching fractions are measured:

$$\frac{\mathcal{B}(B_s^0 \to \chi_{c1}\phi)}{\mathcal{B}(B_s^0 \to J/\psi\phi)} = \left(18.9 \pm 1.8\,(\text{stat})\ \pm 1.3\,(\text{syst})\ \pm 0.8(\mathcal{B})\right) \times 10^{-2},$$

$$\frac{\mathcal{B}(B^0 \to \chi_{c1}K^{*0})}{\mathcal{B}(B^0 \to J/\psi K^{*0})} = \left(19.8 \pm 1.1\,(\text{stat})\ \pm 1.2\,(\text{syst})\ \pm 0.9(\mathcal{B})\right) \times 10^{-2},$$

$$\frac{\mathcal{B}(B^0 \to \chi_{c2}K^{*0})}{\mathcal{B}(B^0 \to \chi_{c1}K^{*0})} = \left(17.1\ \pm 5.0\,(\text{stat}) \pm 1.7\,(\text{syst}) \pm 1.1(\mathcal{B})\right) \times 10^{-2},$$

where the third uncertainty is due to the limited knowledge of the branching fractions of $\chi_c \to J/\psi\gamma$ modes.

1. Introduction

Two-body B-meson decays into a final states containing charmonium meson have played a crucial role in the observation of CP violation in the B-meson system. These decay modes also provide a sensitive laboratory for studying the effects of the strong interaction. Such decays are expected to proceed predominantly via the colour-suppressed tree diagram involving $\bar{b} \to \bar{c}c\bar{s}$ transition shown in Fig. 1. Under the factorization hypothesis the branching ratios of the $B_{(s)}^0 \to \chi_{c0,2}X$ decays, where X denotes a K^{*0} or a ϕ meson, are expected to be small
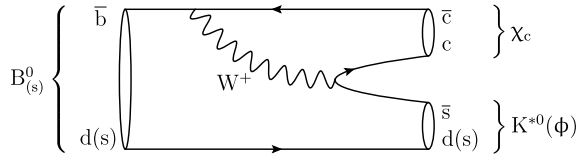

Fig. 1. Leading-order tree level diagram for the $B^0_{(s)} \to \chi_c X$ decays.

in comparison to $B^0_{(s)} \to \chi_{c1} X$ decays [1]. However, non-factorizable contributions may be large [1]; the branching fraction for the $B^0 \to \chi_{c0} K^{*0}$ decay was measured by the BaBar Collaboration to be $(1.7 \pm 0.3 \pm 0.2) \times 10^{-4}$ [2] while the branching fraction for the $B^0 \to \chi_{c1} K^{*0}$ decay was measured by the BaBar and Belle Collaborations to be $(2.5 \pm 0.2 \pm 0.2) \times 10^{-4}$ [3] and $(1.73^{+0.15+0.34}_{-0.12-0.22}) \times 10^{-4}$ [4], respectively. The branching fraction for the decay $B^0 \to \chi_{c2} K^{*0}$ has been measured by the BaBar Collaboration to be $(6.6 \pm 1.8 \pm 0.5) \times 10^{-5}$ [3] and, unlike the branching fraction for the $B^0 \to \chi_{c0} K^{*0}$ decay, can still be explained in the factorization approach [5]. Therefore, future measurements of the branching fractions of both $B^0 \to \chi_{c1} K^{*0}$ and $B^0 \to \chi_{c2} K^{*0}$ decays can provide valuable information for the understanding of the production of χ_c states in B meson decays, where χ_c denotes χ_{c1} and χ_{c2} states. The decay modes $B^0_s \to \chi_c \phi$ have not been observed previously.

In this paper, the first observation of the decay $B^0_s \to \chi_{c1} \phi$ and a study of the $B^0 \to \chi_{c1,2} K^{*0}$ decays are presented. The analysis is based on a data sample, corresponding to an integrated luminosity of 1.0 fb^{-1}, collected with the LHCb detector in pp collisions at a centre-of-mass energy of 7 TeV.

2. LHCb detector

The LHCb detector [6] is a single-arm forward spectrometer covering the pseudorapidity range $2 < \eta < 5$, designed for the study of particles containing b or c quarks. The detector includes a high precision tracking system consisting of a silicon-strip vertex detector surrounding the pp interaction region, a large-area silicon-strip detector located upstream of a dipole magnet with a bending power of about 4 Tm, and three stations of silicon-strip detectors and straw drift tubes placed downstream. The combined tracking system has momentum resolution $\Delta p / p$ that varies from 0.4% at 5 GeV/c to 0.6% at 100 GeV/c, and impact parameter resolution of 20 μm for tracks with high transverse momentum (p_T). Charged hadrons are identified using two ring-imaging Cherenkov detectors [7]. Photon, electron and hadron candidates are identified by a calorimeter system consisting of scintillating-pad and preshower detectors, an electromagnetic calorimeter and a hadronic calorimeter. Muons are identified by a system composed of alternating layers of iron and multiwire proportional chambers [8].

The trigger [9] consists of a hardware stage, based on information from the calorimeter and muon systems, followed by a software stage where a full event reconstruction is applied. Candidate events are first required to pass a hardware trigger which selects muons with $p_T > 1.48$ GeV/c. In the subsequent software trigger, at least one of the muons is required to have both $p_T > 0.8$ GeV/c and impact parameter larger than 100 μm with respect to all of the primary pp interaction vertices (PVs) in the event. Finally, the two final state muons are required to form a vertex that is significantly displaced from the PVs.

The analysis technique reported below has been validated using simulated events. The pp collisions are generated using PYTHIA 6.4 [10] with a specific LHCb configuration [11]. Decays

of hadronic particles are described by EVTGEN [12] in which final state radiation is generated using PHOTOS [13]. The interaction of the generated particles with the detector and its response are implemented using the GEANT4 toolkit [14,15] as described in Ref. [16].

3. Event selection

The decays $B^0 \to \chi_c K^{*0}$ and $B_s^0 \to \chi_c \phi$ (the inclusion of charged conjugate processes is implied throughout) are reconstructed using the $\chi_c \to J/\psi \gamma$ decay mode. The decays $B^0 \to J/\psi K^{*0}$ and $B_s^0 \to J/\psi \phi$ are used as normalization channels. The intermediate resonances are reconstructed in the $J/\psi \to \mu^+\mu^-$, $K^{*0} \to K^+\pi^-$ and $\phi \to K^+K^-$ final states.

As in Refs. [17–19], pairs of oppositely-charged tracks identified as muons, each having $p_T > 0.55$ GeV/c and originating from a common vertex, are combined to form $J/\psi \to \mu^+\mu^-$ candidates. Track quality is ensured by requiring the χ^2 per number of degrees of freedom (χ^2/ndf) provided by the track fit to be less than 5. Well identified muons are selected by requiring that the difference in logarithms of the likelihood of the muon hypothesis with respect to the hadron hypothesis is larger than zero [8]. The fit of the common two-prong vertex is required to satisfy χ^2/ndf < 20. The vertex is required to be well separated from the reconstructed primary vertex of any of the pp interactions by requiring the decay length to be at least three times its uncertainty. Finally, the invariant mass of the dimuon combination is required to be between 3.020 and 3.135 GeV/c^2.

To create χ_c candidates, the selected J/ψ candidates are combined with a photon that has been reconstructed using clusters in the electromagnetic calorimeter that have transverse energy greater than 0.7 GeV. To suppress the large combinatorial background from $\pi^0 \to \gamma\gamma$ decays, photons that can form part of a $\pi^0 \to \gamma\gamma$ candidate with invariant mass within 10 MeV/c^2 of the known π^0 mass [20] are not used for reconstruction of χ_c candidates. To be considered as a χ_c, the $J/\psi\gamma$ combination needs to have a transverse momentum larger than 3 GeV/c and an invariant mass in the range 3.4–3.7 GeV/c^2.

The selected χ_c and J/ψ candidates are then combined with $K^+\pi^-$ or K^+K^- pairs to create $B_{(s)}^0$ meson candidates. To identify kaons (pions), the difference in logarithm of the likelihood of the kaon and pion hypotheses [7] is required to be greater than (less than) zero. The track χ^2/ndf provided by the track fit is required to be less than 5. The kaons and pions are required to have transverse momentum larger than 0.8 GeV/c and to have an impact parameter χ^2, defined as the difference between the χ^2 of the reconstructed pp collision vertex formed with and without the considered track, larger than 4. The invariant mass of the kaon and pion system, $M_{K^+\pi^-}$, is required to be $0.675 < M_{K^+\pi^-} < 1.215$ GeV/c^2 and the invariant mass of the kaon pair, $M_{K^+K^-}$, is required to be $0.999 < M_{K^+K^-} < 1.051$ GeV/c^2. In the reconstruction of K^{*0} candidates, a possible background arises from $\phi \to K^+K^-$ decays when a kaon is misidentified as a pion. To suppress this contribution, the invariant mass of the kaon and pion system, calculated under the kaon mass hypothesis for the pion track, is required to be outside the range from 1.01 to 1.03 GeV/c^2.

In addition, the decay time of B candidates is required to be larger than 150 μm/c to reduce the large combinatorial background from particles produced in the primary pp interaction. To improve the invariant mass resolution of the $B_{(s)}^0$ meson candidate a kinematic fit [21] is performed. In this fit, constraints are applied to the masses of the intermediate J/ψ and χ_c resonances [20] and it is also required that the $B_{(s)}^0$ meson candidate momentum vector points to the primary vertex. The χ^2/ndf for this fit is required to be less than 5.

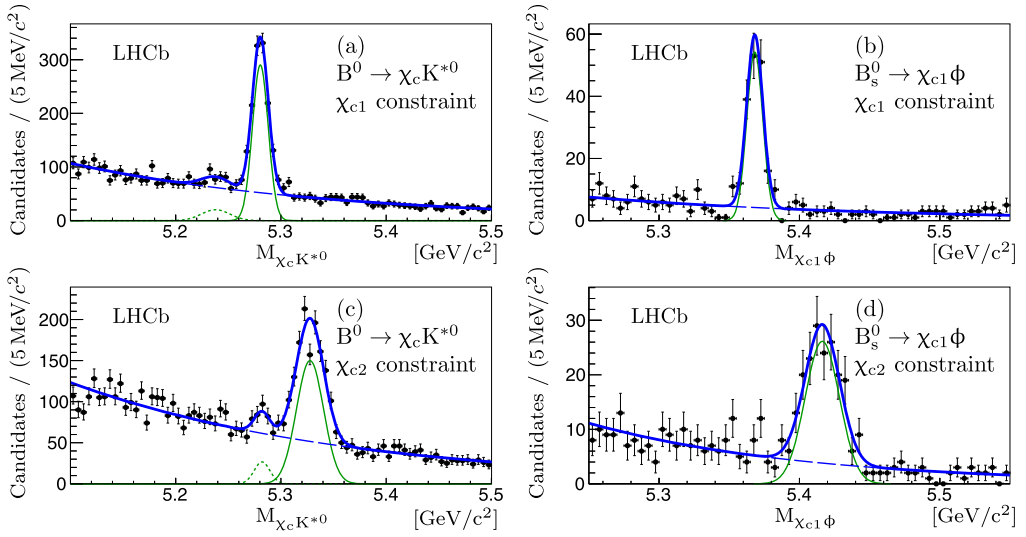Fig. 2. Invariant mass distributions for: (a) $B^0 \to \chi_c K^{*0}$ and (b) $B_s^0 \to \chi_{c1}\phi$ candidates with χ_{c1} mass constraint; (c) $B^0 \to \chi_c K^{*0}$ and (d) $B_s^0 \to \chi_{c1}\phi$ candidates with χ_{c2} mass constraint. The total fitted function (thick solid blue), signal for the χ_{c1} and χ_{c2} modes (thin green solid and dotted, respectively) and the combinatorial background (dashed blue) are shown.

4. $B^0 \to \chi_c K^{*0}$ and $B_s^0 \to \chi_{c1}\phi$ decays

The invariant mass distributions after selecting $B^0 \to \chi_c K^{*0}$ and $B_s^0 \to \chi_{c1}\phi$ candidates, separately with a χ_{c1} and χ_{c2} mass constraints, are shown in Fig. 2. The signal is modelled by a single Gaussian function and the combinatorial background is modelled by an exponential function. In the B^0 channel (Figs. 2(a) and (c)), the right peak in the mass distributions corresponds to the χ_{c1} mode and the left one to the χ_{c2} mode. Owing to the small $\chi_{c0} \to J/\psi\gamma$ branching fraction [20] the contribution from the χ_{c0} mode is negligible. As the B^0 candidate mass is calculated with the $J/\psi\gamma$ invariant mass constrained to the χ_{c1} (χ_{c2}) known mass, the signal peak corresponding to the χ_{c2} (χ_{c1}) mode is shifted to a lower (higher) value with respect to the B^0 mass. The same effect is observed in simulation. The ratio of the mass resolutions of these two signal peaks is fixed to the value obtained from simulation. In the B_s^0 channel no significant contribution from the χ_{c2} decay mode is expected and therefore it is not considered in the fit. The statistical significance for the observed signal is determined as $S = \sqrt{-2\ln\frac{\mathcal{L}_B}{\mathcal{L}_{S+B}}}$, where $\mathcal{L}_{S+B}$ and $\mathcal{L}_B$ denote the likelihood of the signal plus background hypothesis and the background only hypothesis, respectively. The statistical significance of the $B_s^0 \to \chi_{c1}\phi$ signal is found to be larger than 9 standard deviations.

The positions and resolutions of the signal peaks are consistent with the expectations from simulation. To investigate the different signal yields obtained with the χ_{c1} and χ_{c2} mass constraints, a simplified simulation study was performed, which accounts for correlations, differences in selection efficiencies and background fluctuations. This study demonstrates that the yields are in agreement within the statistical uncertainty.

To examine the resonance structure of the $B^0 \to \chi_c K^{*0}$ and $B_s^0 \to \chi_{c1}\phi$ decays, the *sPlot* technique [22] was used with weights determined from the $B_{(s)}^0$ candidate invariant mass fits described above. The invariant mass distributions for each signal component are obtained. For the
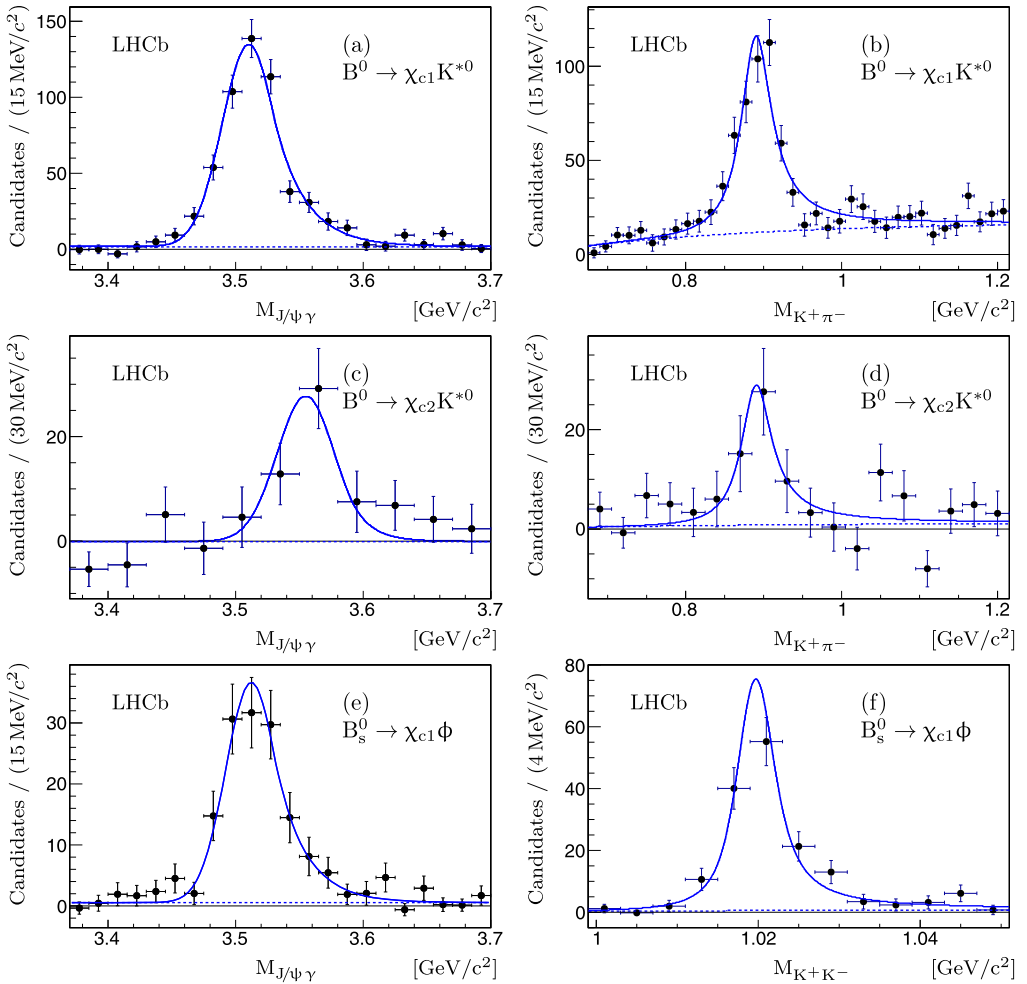
Fig. 3. Background-subtracted invariant mass distributions for: (a) $J/\psi\gamma$ and (b) $K^+\pi^-$ final states from $B^0 \to \chi_{c1}K^{*0}$ decays obtained with the χ_{c1} mass constraint applied to the $B^0_{(s)}$ candidate invariant mass; (c) $J/\psi\gamma$ and (d) $K^+\pi^-$ final states from $B^0 \to \chi_{c2}K^{*0}$ decays obtained with the χ_{c2} mass constraint applied to the $B^0_{(s)}$ candidate invariant mass; (e) $J/\psi\gamma$ and (f) K^+K^- final states from $B^0_s \to \chi_{c1}\phi$ decays obtained with the χ_{c1} mass constraint applied to the $B^0_{(s)}$ candidate invariant mass. The total fitted function (solid) and the non-resonant contribution (dotted) are shown.

$J/\psi\gamma$ invariant mass distributions the requirement on the invariant mass of the $K^+\pi^-(K^+K^-)$ system is tightened to be within 50(10) MeV/c^2 around the known $K^{*0}(\phi)$ mass to reduce background.

The resulting invariant mass distributions for $J/\psi\gamma$, $K^+\pi^-$ and K^+K^- from $B^0 \to \chi_c K^{*0}$ and $B^0_s \to \chi_{c1}\phi$ candidates are shown in Fig. 3. The $J/\psi\gamma$ invariant mass distributions are modelled with the sum of a constant and a Crystal Ball function [23] with tail parameters fixed to simulation. In the χ_{c2} mode the signal peak position is fixed to the sum of the χ_{c1} peak position and the known difference between χ_{c1} and χ_{c2} masses [20]. The χ_{c2} mass resolution is fixed to the χ_{c1} mass resolution multiplied by a scale factor determined using simulation. The

Table 1
Signal yields for the B decays.

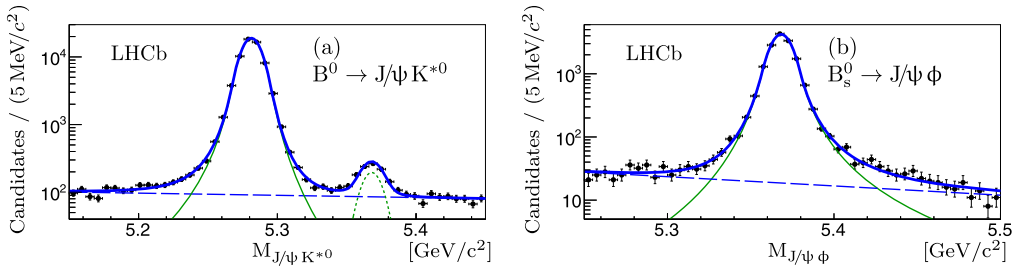| Decay	Yield
$B^0 \to \chi_{c1}K^{*0}$	566 ± 31
$B^0 \to \chi_{c2}K^{*0}$	66 ± 19
$B_s^0 \to \chi_{c1}\phi$	146 ± 14
$B^0 \to J/\psi K^{*0}$	$56,707 \pm 279$
$B_s^0 \to J/\psi\phi$	$15,027 \pm 139$

Fig. 4. Invariant mass distributions for (a) $B^0 \to J/\psi K^{*0}$ and (b) $B_s^0 \to J/\psi\phi$. The total fitted function (thick solid blue), signal (thin solid green), the $B_s^0 \to J/\psi K^{*0}$ (green dotted) and the combinatorial background (dashed blue) are shown.

$K^+\pi^-$ and K^+K^- invariant mass distributions are modelled with the sum of a relativistic P-wave Breit–Wigner function with the natural width fixed to the known value [20] and a non-resonant component modelled with the LASS parametrization [24]. For the K^+K^- case the relativistic P-wave Breit–Wigner function is convolved with a Gaussian function for the detector resolution.

The signal peak positions are consistent with the known masses of the mesons while the invariant mass resolutions are consistent with the expectation from simulation. In the $J/\psi\gamma$ invariant mass distributions, the non-resonant contribution is consistent with zero. The resonant contributions for the $B^0 \to \chi_{c1}K^{*0}$ and $B_s^0 \to \chi_{c1}\phi$ decays are determined with the χ_{c1} mass constraint while the resonant contribution for the $B^0 \to \chi_{c2}K^{*0}$ decay is determined with the χ_{c2} mass constraint. The resulting resonant yields, obtained from the fits to the background-subtracted $K^+\pi^-$ and K^+K^- distributions, are shown in Table 1.

5. $B^0 \to J/\psi K^{*0}$ and $B_s^0 \to J/\psi\phi$ decays

The $B^0 \to \chi_c K^{*0}$ and $B_s^0 \to \chi_{c1}\phi$ branching fractions are measured with respect to the $B^0 \to J/\psi K^{*0}$ and $B_s^0 \to J/\psi\phi$ decays to reduce the systematic uncertainties. The invariant mass distributions for the $B^0 \to J/\psi K^{*0}$ and $B_s^0 \to J/\psi\phi$ candidates after selection requirements are shown in Fig. 4. The signal and the $B_s^0 \to J/\psi K^{*0}$ invariant mass distributions are modelled by a double-sided Crystal Ball function and the combinatorial background is modelled by an exponential function. The parameters of the B_s^0 peak are fixed to be the same as those of the B^0 peak except the position and yield. The difference between the $B^0 \to J/\psi K^{*0}$ and $B_s^0 \to J/\psi K^{*0}$ peak positions is fixed to the world average [20]. The positions of the signal peaks are consistent with the known masses of the $B_{(s)}^0$ mesons [20] and the mass resolutions are consistent with expectations from simulation.

The resonant contributions in the $B^0 \to J/\psi K^{*0}$ and $B_s^0 \to J/\psi\phi$ decays are determined using the *sPlot* technique with the same method as that used for the $B^0 \to \chi_c K^{*0}$ and $B_s^0 \to \chi_c\phi$
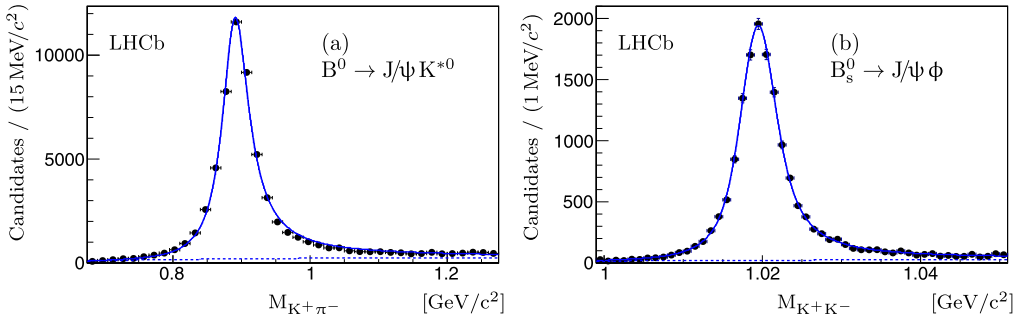
Fig. 5. Background-subtracted invariant mass distributions for (a) $K^+\pi^-$ combinations from $B^0 \to J/\psi K^{*0}$ decays and (b) K^+K^- combination from $B_s^0 \to J/\psi\phi$ decays. The total fitted function (solid) and the non-resonant contribution (dotted) are shown.

Table 2
Total efficiencies for all decay modes. Uncertainties are statistical only and reflect the size of the simulation sample.

Decay	Efficiency [10^{-4}]
$B^0 \to \chi_{c1}K^{*0}$	7.89 ± 0.12
$B^0 \to \chi_{c2}K^{*0}$	9.45 ± 0.13
$B_s^0 \to \chi_{c1}\phi$	12.7 ± 0.2
$B^0 \to J/\psi K^{*0}$	53.9 ± 0.3
$B_s^0 \to J/\psi\phi$	85.1 ± 0.4

decays. The resulting $K^+\pi^-$ and K^+K^- invariant mass distributions from $B^0 \to J/\psi K^{*0}$ and $B_s^0 \to J/\psi\phi$ candidates are shown in Fig. 5. The resulting resonant yields are summarized in Table 1. The S-wave contributions are consistent with those considered in other analyses [17,25,26].

6. Efficiencies and systematic uncertainties

The branching fraction ratios are calculated using the formulas

$$\frac{\mathcal{B}(B \to \chi_{c1}X)}{\mathcal{B}(B \to J/\psi X)} = \frac{N_{B \to \chi_{c1}X}}{N_{B \to J/\psi X}} \times \frac{\varepsilon_{B \to J/\psi X}}{\varepsilon_{B \to \chi_{c1}X}} \times \frac{1}{\mathcal{B}(\chi_{c1} \to J/\psi\gamma)},$$

$$\frac{\mathcal{B}(B \to \chi_{c2}X)}{\mathcal{B}(B \to \chi_{c1}X)} = \frac{N_{B \to \chi_{c2}X}}{N_{B \to \chi_{c1}X}} \times \frac{\varepsilon_{B \to \chi_{c1}X}}{\varepsilon_{B \to \chi_{c2}X}} \times \frac{\mathcal{B}(\chi_{c1} \to J/\psi\gamma)}{\mathcal{B}(\chi_{c2} \to J/\psi\gamma)}, \qquad (1)$$

where N represents the measured yield and ε represents the total efficiency. The total efficiency is the product of the geometrical acceptance, the detection, reconstruction, selection and trigger efficiencies. The efficiencies are derived using simulation and are presented in Table 2.

Most potential sources of systematic uncertainty cancel in the ratio, in particular, those related to the muon and J/ψ reconstruction and identification. The remaining systematic uncertainties are summarized in Table 3 and each is now discussed in turn.

Systematic uncertainties related to the signal determination procedure are estimated using a number of alternative options. For each of the alternatives the ratio of event yields is calculated and the systematic uncertainty is then determined as the maximum deviation of this ratio from the ratio obtained with the baseline model. For the $B_{(s)}^0$ meson decays a fit with a second-order

Table 3
Relative systematic uncertainties (in %) on the ratio of branching fractions.

Source	$\frac{\mathcal{B}(B_s^0 \to \chi_{c1}\phi)}{\mathcal{B}(B_s^0 \to J/\psi\phi)}$	$\frac{\mathcal{B}(B^0 \to \chi_{c1}K^{*0})}{\mathcal{B}(B^0 \to J/\psi K^{*0})}$	$\frac{\mathcal{B}(B^0 \to \chi_{c2}K^{*0})}{\mathcal{B}(B^0 \to \chi_{c1}K^{*0})}$
Signal determination	5	3	9
Efficiencies from simulation	3	3	3
Photon reconstruction	4	4	–
Trigger	1	1	1
Sum in quadrature	7	6	10

polynomial for the combinatorial background description, a fit with a Crystal Ball [23] function for the signal peaks and fit over different ranges of invariant mass are used. In the B_s^0 channel a fit including the χ_{c2} decay mode is also performed. For the $K^+\pi^-$ and K^+K^- combinations the fits are repeated, modelling the background with an S-wave two-body phase-space function or an S-wave two-body phase-space function multiplied by a linear function. The $K^+\pi^-$ and K^+K^- invariant mass ranges and the bin size are also varied. The resulting uncertainties are 3% on $\mathcal{B}(B^0 \to \chi_{c1}K^{*0})/\mathcal{B}(B^0 \to J/\psi K^{*0})$, 5% on $\mathcal{B}(B_s^0 \to \chi_{c1}\phi)/\mathcal{B}(B_s^0 \to J/\psi\phi)$, and 9% on $\mathcal{B}(B^0 \to \chi_{c2}K^{*0})/\mathcal{B}(B^0 \to \chi_{c1}K^{*0})$.

Another important source of systematic uncertainty arises from the potential disagreement between data and simulation in the estimation of efficiencies. To study this source of uncertainty, the selection criteria are varied in ranges corresponding to as much as 30% change in the signal yields and the ratios of the selection and reconstruction efficiencies are compared between data and simulation. The largest difference (3%) is assigned as a systematic uncertainty in each mode.

A further source of possible disagreement between data and simulation is the photon reconstruction efficiency. As in Ref. [18], the photon reconstruction efficiency has been studied using $B^+ \to J/\psi K^{*+}$, followed by $K^{*+} \to K^+\pi^0$ and $\pi^0 \to \gamma\gamma$ decays. For photons with transverse momentum greater than $0.7\,\text{GeV}/c$ the agreement between data and simulation is at the level of 4%, which is assigned as a systematic uncertainty to the ratios $\mathcal{B}(B^0 \to \chi_{c1}K^{*0})/\mathcal{B}(B^0 \to J/\psi K^{*0})$ and $\mathcal{B}(B_s^0 \to \chi_{c1}\phi)/\mathcal{B}(B_s^0 \to J/\psi\phi)$. As the transverse momentum spectra of photons are similar in $B^0 \to \chi_{c1}K^{*0}$ and $B^0 \to \chi_{c2}K^{*0}$ decays, this systematic uncertainty cancels in the ratio $\mathcal{B}(B^0 \to \chi_{c2}K^{*0})/\mathcal{B}(B^0 \to \chi_{c1}K^{*0})$.

The systematic uncertainty related to the trigger efficiency has been obtained by comparing the trigger efficiency ratios in data and simulation for the high yield decay modes $B^+ \to J/\psi K^+$ and $B^+ \to \psi(2S)K^+$ which have similar kinematics and the same trigger requirements as the channels under study in this analysis [17]. An agreement within 1% is found, which is assigned as systematic uncertainty.

The uncertainty due to the finite simulation sample size is included in the statistical uncertainty of the result by adding it in quadrature to the statistical uncertainty on the ratio of yields.

7. Results and summary

The first observation of the $B_s^0 \to \chi_{c1}\phi$ decay has been made with a data sample, corresponding to an integrated luminosity of $1.0\,\text{fb}^{-1}$ of pp collisions at a centre-of-mass energy of 7 TeV, collected with the LHCb detector. Its branching fraction, normalized to that of the $B_s^0 \to J/\psi\phi$ decay and using the known value $\mathcal{B}(\chi_{c1} \to J/\psi\gamma) = (34.4 \pm 1.5)\%$ [20], is measured to be

$$\frac{\mathcal{B}(B_s^0 \to \chi_{c1}\phi)}{\mathcal{B}(B_s^0 \to J/\psi\phi)} = \left(6.51 \pm 0.64\,(\text{stat}) \pm 0.46\,(\text{syst})\right) \times 10^{-2} \times \frac{1}{\mathcal{B}(\chi_{c1} \to J/\psi\gamma)}$$

$$= \left(18.9 \pm 1.8\,(\text{stat}) \pm 1.3\,(\text{syst}) \pm 0.8\,(\mathcal{B})\right) \times 10^{-2},$$

where the third uncertainty corresponds to the uncertainty on the branching fraction of the $\chi_{c1} \to J/\psi\gamma$ decay. Using the same dataset, the ratio of the branching fractions of the $B^0 \to \chi_{c1}K^{*0}$ and $B^0 \to J/\psi K^{*0}$ modes and the ratio of the branching fractions of the $B^0 \to \chi_{c2}K^{*0}$ and $B^0 \to \chi_{c1}K^{*0}$ modes have been measured. The ratios are determined using Eq. (1) and the known value $\frac{\mathcal{B}(\chi_{c1} \to J/\psi\gamma)}{\mathcal{B}(\chi_{c2} \to J/\psi\gamma)} = \frac{(34.4\pm1.5)\%}{(19.5\pm0.8)\%} = 1.76 \pm 0.11$ [20] and are

$$\frac{\mathcal{B}(B^0 \to \chi_{c1}K^{*0})}{\mathcal{B}(B^0 \to J/\psi K^{*0})} = \left(6.82 \pm 0.39\,(\text{stat}) \pm 0.41\,(\text{syst})\right) \times 10^{-2} \times \frac{1}{\mathcal{B}(\chi_{c1} \to J/\psi\gamma)}$$

$$= \left(19.8 \pm 1.1\,(\text{stat}) \pm 1.2\,(\text{syst}) \pm 0.9\,(\mathcal{B})\right) \times 10^{-2},$$

$$\frac{\mathcal{B}(B^0 \to \chi_{c2}K^{*0})}{\mathcal{B}(B^0 \to \chi_{c1}K^{*0})} = \left(9.74 \pm 2.86\,(\text{stat}) \pm 0.97\,(\text{syst})\right) \times 10^{-2} \times \frac{\mathcal{B}(\chi_{c1} \to J/\psi\gamma)}{\mathcal{B}(\chi_{c2} \to J/\psi\gamma)}$$

$$= \left(17.1 \pm 5.0\,(\text{stat}) \pm 1.7\,(\text{syst}) \pm 1.1\,(\mathcal{B})\right) \times 10^{-2},$$

where the third uncertainty is due to the uncertainty on the branching fractions of the $\chi_c \to J/\psi\gamma$ modes.

The ratio $\mathcal{B}(B^0 \to \chi_{c1}K^{*0})/\mathcal{B}(B^0 \to J/\psi K^{*0})$ obtained in this paper is compatible with, but more precise than, the previous best value of $(17.2^{+3.6}_{-3.0}) \times 10^{-2}$ determined from the world average value $\mathcal{B}(B^0 \to \chi_{c1}K^{*0}) = (2.22^{+0.40}_{-0.31}) \times 10^{-4}$ [20] and the branching fraction $\mathcal{B}(B^0 \to J/\psi K^{*0}) = (1.29 \pm 0.05 \pm 0.13) \times 10^{-3}$ measured by the Belle Collaboration [27]. Other measurements of $\mathcal{B}(B^0 \to J/\psi K^{*0})$ are not considered as they do not take into account the $K^+\pi^-$ S-wave component. The ratio $\mathcal{B}(B^0 \to \chi_{c2}K^{*0})/\mathcal{B}(B^0 \to \chi_{c1}K^{*0})$ obtained in this paper is compatible with the value derived from BaBar measurements, $(26 \pm 7(\text{stat})) \times 10^{-2}$ [3], taking only the statistical uncertainties into account.

References

[1] C. Meng, Y.-J. Gao, K.-T. Chao, Puzzles in B → h$_c$(χ$_{c2}$)K decays and QCD factorization, arXiv:hep-ph/0607221.

[2] BaBar Collaboration, B. Aubert, et al., Observation of B^0 → χ$_{c0}$K^{*0} and evidence for B$^+$ → χ$_{c0}$K^{*+}, Phys. Rev. D 78 (2008) 091101, arXiv:0808.1487.

[3] BaBar Collaboration, B. Aubert, et al., Evidence for X(3872) → ψ(2S)γ in B$^\pm$ → X(3872)K$^\pm$ decays, and a study of B → cc̄γK, Phys. Rev. Lett. 102 (2009) 132001, arXiv:0809.0042.

[4] Belle Collaboration, R. Mizuk, et al., Observation of two resonance-like structures in the π$^\pm$χ$_{c1}$ mass distribution in exclusive B̄^{0} → K$^-$π$^+$χ$_{c1}$ decays, Phys. Rev. D 78 (2008) 072004, arXiv:0806.4098.

[5] M. Beneke, L. Vernazza, B → χ$_{cJ}$K decays revisited, Nucl. Phys. B 811 (2009) 155, arXiv:0810.3575.

[6] LHCb Collaboration, A.A. Alves, et al., The LHCb detector at the LHC, JINST 3 (2008) S08005.

[7] M. Adinolfi, et al., Performance of the LHCb RICH detector at the LHC, Eur. Phys. J. C 73 (2013) 2431, arXiv:1211.6759.

[8] A.A. Alves, et al., Performance of the LHCb muon system, JINST 8 (2013) P02022, arXiv:1211.1346.

[9] R. Aaij, et al., The LHCb trigger and its performance in 2011, JINST 8 (2013) P04022, arXiv:1211.3055.

[10] T. Sjöstrand, S. Mrenna, P. Skands, PYTHIA 6.4 physics and manual, JHEP 0605 (2006) 026, arXiv:hep-ph/0603175.

[11] I. Belyaev, et al., Handling of the generation of primary events in GAUSS, the LHCb simulation framework, in: Nuclear Science Symposium Conference Record (NSS/MIC), IEEE, 2010, p. 1155.

[12] D.J. Lange, The EVTGEN particle decay simulation package, Nucl. Instrum. Meth. A 462 (2001) 152.

[13] P. Golonka, Z. Was, PHOTOS Monte Carlo: a precision tool for QED corrections in Z and W decays, Eur. Phys. J. C 45 (2006) 97, arXiv:hep-ph/0506026.

[14] GEANT4 Collaboration, S. Agostinelli, et al., GEANT4: A simulation toolkit, Nucl. Instrum. Meth. A 506 (2003) 250.

[15] GEANT4 Collaboration, J. Allison, et al., GEANT4 developments and applications, IEEE Trans. Nucl. Sci. 53 (2006) 270.

[16] M. Clemencic, et al., The LHCb simulation application, GAUSS: design, evolution and experience, J. Phys. Conf. Ser. 331 (2011) 032023.

[17] LHCb Collaboration, R. Aaij, et al., Measurement of relative branching fractions of B decays to ψ(2S) and J/ψ mesons, Eur. Phys. J. C 72 (2012) 2118, arXiv:1205.0918.

[18] LHCb Collaboration, R. Aaij, et al., Evidence for the decay B^0 → J/ψω and measurement of the relative branching fractions of B^0_s meson decays to J/ψη and J/ψη′, Nucl. Phys. B 867 (2013) 547, arXiv:1210.2631.

[19] LHCb Collaboration, R. Aaij, et al., Observation of the B^0_s → ψ(2S)η and B^0_s → ψ(2S)π$^+$π$^-$ decays, Nucl. Phys. B 871 (2013) 403, arXiv:1302.6354.

[20] Particle Data Group, J. Beringer, et al., Phys. Rev. D 86 (2012) 010001.

[21] W.D. Hulsbergen, Decay chain fitting with a Kalman filter, Nucl. Instrum. Meth. A 552 (2005) 566, arXiv:physics/0503191.

[22] M. Pivk, F.R. Le, Diberder, sPlot: a statistical tool to unfold data distributions, Nucl. Instrum. Meth. A 555 (2005) 356, arXiv:physics/0402083.

[23] T. Skwarnicki, A study of the radiative cascade transitions between the Upsilon-prime and Upsilon resonances, PhD thesis, Institute of Nuclear Physics, Krakow, 1986.

[24] D. Aston, et al., A study of K$^-$π$^+$ scattering in the reaction K$^-$π$^+$ → K$^-$π$^+$n at 11 GeV/c, Nucl. Phys. B 296 (1988) 493.

[25] LHCb Collaboration, R. Aaij, et al., Measurement of the B^0_s → J/ψK̄^{*0} branching fraction and angular amplitudes, Phys. Rev. D 86 (2012) 071102, arXiv:1208.0738.

[26] LHCbcollaboration, R. Aaij, et al., Measurement of CP violation and the B^0_s-meson decay width difference with B^0_s → J/ψK$^+$K$^-$ and B^0_s → J/ψπ$^+$π$^-$ decays, Phys. Rev. D 87 (2013) 112010, arXiv:1304.2600.

[27] Belle Collaboration, K. Abe, et al., Measurements of branching fractions and decay amplitudes in B → J/ψK* decays, Phys. Lett. B 538 (2002) 11, arXiv:hep-ex/0205021.

LHCb Collaboration

R. Aaij [40], B. Adeva [36], M. Adinolfi [45], C. Adrover [6], A. Affolder [51],
Z. Ajaltouni [5], J. Albrecht [9], F. Alessio [37], M. Alexander [50], S. Ali [40],
G. Alkhazov [29], P. Alvarez Cartelle [36], A.A. Alves Jr [24,37], S. Amato [2],
S. Amerio [21], Y. Amhis [7], L. Anderlini [17,f], J. Anderson [39],
R. Andreassen [56], J.E. Andrews [57], R.B. Appleby [53],
O. Aquines Gutierrez [10], F. Archilli [18], A. Artamonov [34], M. Artuso [58],
E. Aslanides [6], G. Auriemma [24,m], M. Baalouch [5], S. Bachmann [11],
J.J. Back [47], C. Baesso [59], V. Balagura [30], W. Baldini [16], R.J. Barlow [53],
C. Barschel [37], S. Barsuk [7], W. Barter [46], Th. Bauer [40], A. Bay [38],
J. Beddow [50], F. Bedeschi [22], I. Bediaga [1], S. Belogurov [30], K. Belous [34],
I. Belyaev [30,*], E. Ben-Haim [8], G. Bencivenni [18], S. Benson [49], J. Benton [45],
A. Berezhnoy [31], R. Bernet [39], M.-O. Bettler [46], M. van Beuzekom [40],
A. Bien [11], S. Bifani [44], T. Bird [53], A. Bizzeti [17,h], P.M. Bjørnstad [53],
T. Blake [37], F. Blanc [38], J. Blouw [11], S. Blusk [58], V. Bocci [24], A. Bondar [33],
N. Bondar [29], W. Bonivento [15], S. Borghi [53], A. Borgia [58],
T.J.V. Bowcock [51], E. Bowen [39], C. Bozzi [16], T. Brambach [9],
J. van den Brand [41], J. Bressieux [38], D. Brett [53], M. Britsch [10], T. Britton [58],
N.H. Brook [45], H. Brown [51], I. Burducea [28], A. Bursche [39], G. Busetto [21,q],
J. Buytaert [37], S. Cadeddu [15], O. Callot [7], M. Calvi [20,j],
M. Calvo Gomez [35,n], A. Camboni [35], P. Campana [18,37],
D. Campora Perez [37], A. Carbone [14,c], G. Carboni [23,k], R. Cardinale [19,i],
A. Cardini [15], H. Carranza-Mejia [49], L. Carson [52], K. Carvalho Akiba [2],
G. Casse [51], L. Castillo Garcia [37], M. Cattaneo [37], Ch. Cauet [9], R. Cenci [57],
M. Charles [54], Ph. Charpentier [37], P. Chen [3,38], N. Chiapolini [39],
M. Chrzaszcz [25], K. Ciba [37], X. Cid Vidal [37], G. Ciezarek [52],
P.E.L. Clarke [49], M. Clemencic [37], H.V. Cliff [46], J. Closier [37], C. Coca [28],
V. Coco [40], J. Cogan [6], E. Cogneras [5], P. Collins [37],
A. Comerma-Montells [35], A. Contu [15,37], A. Cook [45], M. Coombes [45],
S. Coquereau [8], G. Corti [37], B. Couturier [37], G.A. Cowan [49], D.C. Craik [47],
S. Cunliffe [52], R. Currie [49], C. D'Ambrosio [37], P. David [8], P.N.Y. David [40],
A. Davis [56], I. De Bonis [4], K. De Bruyn [40], S. De Capua [53], M. De Cian [39],
J.M. De Miranda [1], L. De Paula [2], W. De Silva [56], P. De Simone [18],
D. Decamp [4], M. Deckenhoff [9], L. Del Buono [8], N. Déléage [4],
D. Derkach [54], O. Deschamps [5], F. Dettori [41], A. Di Canto [11],
F. Di Ruscio [23,k], H. Dijkstra [37], M. Dogaru [28], S. Donleavy [51], F. Dordei [11],
A. Dosil Suárez [36], D. Dossett [47], A. Dovbnya [42], F. Dupertuis [38],

R. Dzhelyadin [34], A. Dziurda [25], A. Dzyuba [29], S. Easo [48,37], U. Egede [52],
V. Egorychev [30], S. Eidelman [33], D. van Eijk [40], S. Eisenhardt [49],
U. Eitschberger [9], R. Ekelhof [9], L. Eklund [50,37], I. El Rifai [5],
Ch. Elsasser [39], D. Elsby [44], A. Falabella [14,e], C. Färber [11], G. Fardell [49],
C. Farinelli [40], S. Farry [51], V. Fave [38], D. Ferguson [49],
V. Fernandez Albor [36], F. Ferreira Rodrigues [1], M. Ferro-Luzzi [37],
S. Filippov [32], M. Fiore [16], C. Fitzpatrick [37], M. Fontana [10],
F. Fontanelli [19,i], R. Forty [37], O. Francisco [2], M. Frank [37], C. Frei [37],
M. Frosini [17,f], S. Furcas [20], E. Furfaro [23,k], A. Gallas Torreira [36],
D. Galli [14,c], M. Gandelman [2], P. Gandini [58], Y. Gao [3], J. Garofoli [58],
P. Garosi [53], J. Garra Tico [46], L. Garrido [35], C. Gaspar [37], R. Gauld [54],
E. Gersabeck [11], M. Gersabeck [53], T. Gershon [47,37], Ph. Ghez [4],
V. Gibson [46], L. Giubega [28], V.V. Gligorov [37], C. Göbel [59], D. Golubkov [30],
A. Golutvin [52,30,37], A. Gomes [2], H. Gordon [54], M. Grabalosa Gándara [5],
R. Graciani Diaz [35], L.A. Granado Cardoso [37], E. Graugés [35],
G. Graziani [17], A. Grecu [28], E. Greening [54], S. Gregson [46], P. Griffith [44],
O. Grünberg [60], B. Gui [58], E. Gushchin [32], Yu. Guz [34,37], T. Gys [37],
C. Hadjivasiliou [58], G. Haefeli [38], C. Haen [37], S.C. Haines [46], S. Hall [52],
B. Hamilton [57], T. Hampson [45], S. Hansmann-Menzemer [11], N. Harnew [54],
S.T. Harnew [45], J. Harrison [53], T. Hartmann [60], J. He [37], T. Head [37],
V. Heijne [40], K. Hennessy [51], P. Henrard [5], J.A. Hernando Morata [36],
E. van Herwijnen [37], A. Hicheur [1], E. Hicks [51], D. Hill [54], M. Hoballah [5],
M. Holtrop [40], C. Hombach [53], P. Hopchev [4], W. Hulsbergen [40], P. Hunt [54],
T. Huse [51], N. Hussain [54], D. Hutchcroft [51], D. Hynds [50], V. Iakovenko [43],
M. Idzik [26], P. Ilten [12], R. Jacobsson [37], A. Jaeger [11], E. Jans [40], P. Jaton [38],
A. Jawahery [57], F. Jing [3], M. John [54], D. Johnson [54], C.R. Jones [46],
C. Joram [37], B. Jost [37], M. Kaballo [9], S. Kandybei [42], W. Kanso [6],
M. Karacson [37], T.M. Karbach [37], I.R. Kenyon [44], T. Ketel [41], A. Keune [38],
B. Khanji [20], O. Kochebina [7], I. Komarov [38], R.F. Koopman [41],
P. Koppenburg [40], M. Korolev [31], A. Kozlinskiy [40], L. Kravchuk [32],
K. Kreplin [11], M. Kreps [47], G. Krocker [11], P. Krokovny [33], F. Kruse [9],
M. Kucharczyk [20,25,j], V. Kudryavtsev [33], T. Kvaratskheliya [30,37],
V.N. La Thi [38], D. Lacarrere [37], G. Lafferty [53], A. Lai [15], D. Lambert [49],
R.W. Lambert [41], E. Lanciotti [37], G. Lanfranchi [18], C. Langenbruch [37],
T. Latham [47], C. Lazzeroni [44], R. Le Gac [6], J. van Leerdam [40], J.-P. Lees [4],
R. Lefèvre [5], A. Leflat [31], J. Lefrançois [7], S. Leo [22], O. Leroy [6], T. Lesiak [25],
B. Leverington [11], Y. Li [3], L. Li Gioi [5], M. Liles [51], R. Lindner [37],

C. Linn [11], B. Liu [3], G. Liu [37], S. Lohn [37], I. Longstaff [50], J.H. Lopes [2],
N. Lopez-March [38], H. Lu [3], D. Lucchesi [21,q], J. Luisier [38], H. Luo [49],
F. Machefert [7], I.V. Machikhiliyan [4,30], F. Maciuc [28], O. Maev [29,37],
S. Malde [54], G. Manca [15,d], G. Mancinelli [6], U. Marconi [14], R. Märki [38],
J. Marks [11], G. Martellotti [24], A. Martens [8], A. Martín Sánchez [7],
M. Martinelli [40], D. Martinez Santos [41], D. Martins Tostes [2],
A. Massafferri [1], R. Matev [37], Z. Mathe [37], C. Matteuzzi [20], E. Maurice [6],
A. Mazurov [16,32,37,e], B. McSkelly [51], J. McCarthy [44], A. McNab [53],
R. McNulty [12], B. Meadows [56,54], F. Meier [9], M. Meissner [11], M. Merk [40],
D.A. Milanes [8], M.-N. Minard [4], J. Molina Rodriguez [59], S. Monteil [5],
D. Moran [53], P. Morawski [25], A. Mordà [6], M.J. Morello [22,s],
R. Mountain [58], I. Mous [40], F. Muheim [49], K. Müller [39], R. Muresan [28],
B. Muryn [26], B. Muster [38], P. Naik [45], T. Nakada [38], R. Nandakumar [48],
I. Nasteva [1], M. Needham [49], S. Neubert [37], N. Neufeld [37], A.D. Nguyen [38],
T.D. Nguyen [38], C. Nguyen-Mau [38,o], M. Nicol [7], V. Niess [5], R. Niet [9],
N. Nikitin [31], T. Nikodem [11], A. Nomerotski [54], A. Novoselov [34],
A. Oblakowska-Mucha [26], V. Obraztsov [34], S. Oggero [40], S. Ogilvy [50],
O. Okhrimenko [43], R. Oldeman [15,d], M. Orlandea [28],
J.M. Otalora Goicochea [2], P. Owen [52], A. Oyanguren [35], B.K. Pal [58],
A. Palano [13,b], M. Palutan [18], J. Panman [37], A. Papanestis [48],
M. Pappagallo [50], C. Parkes [53], C.J. Parkinson [52], G. Passaleva [17],
G.D. Patel [51], M. Patel [52], G.N. Patrick [48], C. Patrignani [19,i],
C. Pavel-Nicorescu [28], A. Pazos Alvarez [36], A. Pellegrino [40], G. Penso [24,l],
M. Pepe Altarelli [37], S. Perazzini [14,c], E. Perez Trigo [36],
A. Pérez-Calero Yzquierdo [35], P. Perret [5], M. Perrin-Terrin [6], G. Pessina [20],
K. Petridis [52], A. Petrolini [19,i], A. Phan [58], E. Picatoste Olloqui [35],
B. Pietrzyk [4], T. Pilař [47], D. Pinci [24], S. Playfer [49], M. Plo Casasus [36],
F. Polci [8], G. Polok [25], A. Poluektov [47,33], I. Polyakov [30], E. Polycarpo [2],
A. Popov [34], D. Popov [10], B. Popovici [28], C. Potterat [35], A. Powell [54],
J. Prisciandaro [38], A. Pritchard [51], C. Prouve [7], V. Pugatch [43],
A. Puig Navarro [38], G. Punzi [22,r], W. Qian [4], J.H. Rademacker [45],
B. Rakotomiaramanana [38], M.S. Rangel [2], I. Raniuk [42], N. Rauschmayr [37],
G. Raven [41], S. Redford [54], M.M. Reid [47], A.C. dos Reis [1], S. Ricciardi [48],
A. Richards [52], K. Rinnert [51], V. Rives Molina [35], D.A. Roa Romero [5],
P. Robbe [7], E. Rodrigues [53], P. Rodriguez Perez [36], S. Roiser [37],
V. Romanovsky [34], A. Romero Vidal [36], J. Rouvinet [38], T. Ruf [37],
F. Ruffini [22], H. Ruiz [35], P. Ruiz Valls [35], G. Sabatino [24,k],

J.J. Saborido Silva [36], N. Sagidova [29], P. Sail [50], B. Saitta [15,d],
V. Salustino Guimaraes [2], C. Salzmann [39], B. Sanmartin Sedes [36],
M. Sannino [19,i], R. Santacesaria [24], C. Santamarina Rios [36],
E. Santovetti [23,k], M. Sapunov [6], A. Sarti [18,l], C. Satriano [24,m], A. Satta [23],
M. Savrie [16,e], D. Savrina [30,31], P. Schaack [52], M. Schiller [41],
H. Schindler [37], M. Schlupp [9], M. Schmelling [10], B. Schmidt [37],
O. Schneider [38], A. Schopper [37], M.-H. Schune [7], R. Schwemmer [37],
B. Sciascia [18], A. Sciubba [24], M. Seco [36], A. Semennikov [30], I. Sepp [52],
N. Serra [39], J. Serrano [6], P. Seyfert [11], M. Shapkin [34], I. Shapoval [16,42],
P. Shatalov [30], Y. Shcheglov [29], T. Shears [51,37], L. Shekhtman [33],
O. Shevchenko [42], V. Shevchenko [30], A. Shires [52], R. Silva Coutinho [47],
M. Sirendi [46], T. Skwarnicki [58], N.A. Smith [51], E. Smith [54,48], J. Smith [46],
M. Smith [53], M.D. Sokoloff [56], F.J.P. Soler [50], F. Soomro [18], D. Souza [45],
B. Souza De Paula [2], B. Spaan [9], A. Sparkes [49], P. Spradlin [50], F. Stagni [37],
S. Stahl [11], O. Steinkamp [39], S. Stoica [28], S. Stone [58], B. Storaci [39],
M. Straticiuc [28], U. Straumann [39], V.K. Subbiah [37], L. Sun [56],
S. Swientek [9], V. Syropoulos [41], M. Szczekowski [27], P. Szczypka [38,37],
T. Szumlak [26], S. T'Jampens [4], M. Teklishyn [7], E. Teodorescu [28],
F. Teubert [37], C. Thomas [54], E. Thomas [37], J. van Tilburg [11], V. Tisserand [4],
M. Tobin [38], S. Tolk [41], D. Tonelli [37], S. Topp-Joergensen [54], N. Torr [54],
E. Tournefier [4,52], S. Tourneur [38], M.T. Tran [38], M. Tresch [39],
A. Tsaregorodtsev [6], P. Tsopelas [40], N. Tuning [40], M. Ubeda Garcia [37],
A. Ukleja [27], D. Urner [53], A. Ustyuzhanin [52,p], U. Uwer [11], V. Vagnoni [14],
G. Valenti [14], A. Vallier [7], M. Van Dijk [45], R. Vazquez Gomez [18],
P. Vazquez Regueiro [36], C. Vázquez Sierra [36], S. Vecchi [16], J.J. Velthuis [45],
M. Veltri [17,g], G. Veneziano [38], M. Vesterinen [37], B. Viaud [7], D. Vieira [2],
X. Vilasis-Cardona [35,n], A. Vollhardt [39], D. Volyanskyy [10], D. Voong [45],
A. Vorobyev [29], V. Vorobyev [33], C. Voß [60], H. Voss [10], R. Waldi [60],
C. Wallace [47], R. Wallace [12], S. Wandernoth [11], J. Wang [58], D.R. Ward [46],
N.K. Watson [44], A.D. Webber [53], D. Websdale [52], M. Whitehead [47],
J. Wicht [37], J. Wiechczynski [25], D. Wiedner [11], L. Wiggers [40],
G. Wilkinson [54], M.P. Williams [47,48], M. Williams [55], F.F. Wilson [48],
J. Wimberley [57], J. Wishahi [9], M. Witek [25], S.A. Wotton [46], S. Wright [46],
S. Wu [3], K. Wyllie [37], Y. Xie [49,37], Z. Xing [58], Z. Yang [3], R. Young [49],
X. Yuan [3], O. Yushchenko [34], M. Zangoli [14], M. Zavertyaev [10,a], F. Zhang [3],
L. Zhang [58], W.C. Zhang [12], Y. Zhang [3], A. Zhelezov [11], A. Zhokhov [30],
L. Zhong [3], A. Zvyagin [37]

[1] *Centro Brasileiro de Pesquisas Físicas (CBPF), Rio de Janeiro, Brazil*
[2] *Universidade Federal do Rio de Janeiro (UFRJ), Rio de Janeiro, Brazil*
[3] *Center for High Energy Physics, Tsinghua University, Beijing, China*
[4] *LAPP, Université de Savoie, CNRS/IN2P3, Annecy-Le-Vieux, France*
[5] *Clermont Université, Université Blaise Pascal, CNRS/IN2P3, LPC, Clermont-Ferrand, France*
[6] *CPPM, Aix-Marseille Université, CNRS/IN2P3, Marseille, France*
[7] *LAL, Université Paris-Sud, CNRS/IN2P3, Orsay, France*
[8] *LPNHE, Université Pierre et Marie Curie, Université Paris Diderot, CNRS/IN2P3, Paris, France*
[9] *Fakultät Physik, Technische Universität Dortmund, Dortmund, Germany*
[10] *Max-Planck-Institut für Kernphysik (MPIK), Heidelberg, Germany*
[11] *Physikalisches Institut, Ruprecht-Karls-Universität Heidelberg, Heidelberg, Germany*
[12] *School of Physics, University College Dublin, Dublin, Ireland*
[13] *Sezione INFN di Bari, Bari, Italy*
[14] *Sezione INFN di Bologna, Bologna, Italy*
[15] *Sezione INFN di Cagliari, Cagliari, Italy*
[16] *Sezione INFN di Ferrara, Ferrara, Italy*
[17] *Sezione INFN di Firenze, Firenze, Italy*
[18] *Laboratori Nazionali dell'INFN di Frascati, Frascati, Italy*
[19] *Sezione INFN di Genova, Genova, Italy*
[20] *Sezione INFN di Milano Bicocca, Milano, Italy*
[21] *Sezione INFN di Padova, Padova, Italy*
[22] *Sezione INFN di Pisa, Pisa, Italy*
[23] *Sezione INFN di Roma Tor Vergata, Roma, Italy*
[24] *Sezione INFN di Roma La Sapienza, Roma, Italy*
[25] *Henryk Niewodniczanski Institute of Nuclear Physics, Polish Academy of Sciences, Kraków, Poland*
[26] *AGH – University of Science and Technology, Faculty of Physics and Applied Computer Science, Kraków, Poland*
[27] *National Center for Nuclear Research (NCBJ), Warsaw, Poland*
[28] *Horia Hulubei National Institute of Physics and Nuclear Engineering, Bucharest-Magurele, Romania*
[29] *Petersburg Nuclear Physics Institute (PNPI), Gatchina, Russia*
[30] *Institute of Theoretical and Experimental Physics (ITEP), Moscow, Russia*
[31] *Institute of Nuclear Physics, Moscow State University (SINP MSU), Moscow, Russia*
[32] *Institute for Nuclear Research of the Russian Academy of Sciences (INR RAN), Moscow, Russia*
[33] *Budker Institute of Nuclear Physics (SB RAS) and Novosibirsk State University, Novosibirsk, Russia*
[34] *Institute for High Energy Physics (IHEP), Protvino, Russia*
[35] *Universitat de Barcelona, Barcelona, Spain*
[36] *Universidad de Santiago de Compostela, Santiago de Compostela, Spain*
[37] *European Organization for Nuclear Research (CERN), Geneva, Switzerland*
[38] *Ecole Polytechnique Fédérale de Lausanne (EPFL), Lausanne, Switzerland*
[39] *Physik-Institut, Universität Zürich, Zürich, Switzerland*
[40] *Nikhef National Institute for Subatomic Physics, Amsterdam, The Netherlands*
[41] *Nikhef National Institute for Subatomic Physics and VU University Amsterdam, Amsterdam, The Netherlands*
[42] *NSC Kharkiv Institute of Physics and Technology (NSC KIPT), Kharkiv, Ukraine*
[43] *Institute for Nuclear Research of the National Academy of Sciences (KINR), Kyiv, Ukraine*
[44] *University of Birmingham, Birmingham, United Kingdom*
[45] *H.H. Wills Physics Laboratory, University of Bristol, Bristol, United Kingdom*
[46] *Cavendish Laboratory, University of Cambridge, Cambridge, United Kingdom*
[47] *Department of Physics, University of Warwick, Coventry, United Kingdom*
[48] *STFC, Rutherford Appleton Laboratory, Didcot, United Kingdom*
[49] *School of Physics and Astronomy, University of Edinburgh, Edinburgh, United Kingdom*
[50] *School of Physics and Astronomy, University of Glasgow, Glasgow, United Kingdom*
[51] *Oliver Lodge Laboratory, University of Liverpool, Liverpool, United Kingdom*
[52] *Imperial College London, London, United Kingdom*
[53] *School of Physics and Astronomy, University of Manchester, Manchester, United Kingdom*
[54] *Department of Physics, University of Oxford, Oxford, United Kingdom*
[55] *Massachusetts Institute of Technology, Cambridge, MA, United States*

[56] *University of Cincinnati, Cincinnati, OH, United States*

[57] *University of Maryland, College Park, MD, United States*

[58] *Syracuse University, Syracuse, NY, United States*

[59] *Pontifícia Universidade Católica do Rio de Janeiro (PUC-Rio), Rio de Janeiro, Brazil [t]*

[60] *Institut für Physik, Universität Rostock, Rostock, Germany [u]*

[*] Corresponding author.

   E-mail address: Ivan.Belyaev@itep.ru (I. Belyaev).

[a] P.N. Lebedev Physical Institute, Russian Academy of Science (LPI RAS), Moscow, Russia.

[b] Università di Bari, Bari, Italy.

[c] Università di Bologna, Bologna, Italy.

[d] Università di Cagliari, Cagliari, Italy.

[e] Università di Ferrara, Ferrara, Italy.

[f] Università di Firenze, Firenze, Italy.

[g] Università di Urbino, Urbino, Italy.

[h] Università di Modena e Reggio Emilia, Modena, Italy.

[i] Università di Genova, Genova, Italy.

[j] Università di Milano Bicocca, Milano, Italy.

[k] Università di Roma Tor Vergata, Roma, Italy.

[l] Università di Roma La Sapienza, Roma, Italy.

[m] Università della Basilicata, Potenza, Italy.

[n] LIFAELS, La Salle, Universitat Ramon Llull, Barcelona, Spain.

[o] Hanoi University of Science, Hanoi, Viet Nam.

[p] Institute of Physics and Technology, Moscow, Russia.

[q] Università di Padova, Padova, Italy.

[r] Università di Pisa, Pisa, Italy.

[s] Scuola Normale Superiore, Pisa, Italy.

[t] Associated to: Universidade Federal do Rio de Janeiro (UFRJ), Rio de Janeiro, Brazil.

[u] Associated to: Physikalisches Institut, Ruprecht-Karls-Universität Heidelberg, Heidelberg, Germany.